Journal of Applied Chemistry JAC http://chemistry.journals.semnan.ac.ir

Preparation of Cu-Zn-Ce-Al Spinel Catalyst for Hydrogen Production in Micro-Channel Reactor and Considering the Geometrical Effects of Micro-Channels on Velocity Distribution

A. Parsaee, A. Eliassi*, M. Ranjbar, E. Kashi
Chemical Technologies Department, Iranian Research Organization for Science and Technology (IROST), Tehran, Iran

Article history:
Received:13/Aug/2017
Received in revised form: 30/Aug/2017
Accepted: 09/Sep/2017

Abstract

In this paper, preparation of new Cu-Zn-Al spinel catalysts with CeO_2 using sol-gel and homogeneous precipitation methods are reported. For evaluation of the prepared catalysts for steam reforming of methanol, an A-type micro-channel reactor was designed and fabricated and the prepared catalysts were coated on the reactor channels by hybrid method between sol-gel and suspension methods. The catalysts were evaluated at 270 ºC to 310 ºC. For the catalysts evaluation a mixture of methanol and water with 1.5, 2.5 and 3.5 molar ratios were used as the feed of the reactor. Flow rate of the feed was 2 cc/h. Obtained results show that the prepared spinel catalysts is an appropriate catalysts for hydrogen production by methanol steam reforming. Also, by computational fluid dynamic the geometrical effects of micro-channels on velocity distribution of gases for two different A-type and Z-type micro-channels were considered.

Keywords: Hydrogen; methanol; steam reforming; micro-channel reactor; spinel catalyst; catalyst coating.

1. Introduction

In a time where the environmental issues are one of the greatest concerns in the world, it is essential to search and develop new sources of clean energy. Environmentally friendly technologies such as fuel cells are encouraging for electricity generation. Recently, fuel cell system has turned a promising candidate for portable power source. Specifically, the polymer electrolyte membrane fuel cell (PEMFC) is a power generation system appropriate for small-scale and transport applications [1].

One of the advantages of the fuel cells is that their emissions are very low, but most of the fuel cells require hydrogen as a fuel, which is extremely hard to store and transport. Reforming of alcohols and hydrocarbons allows a hydrogen production in situ, which solves the previously mentioned problems. Even though methane is currently the main fuel in industrial hydrogen production, other hydrogen carriers such as methanol can be used for this purpose. In compared with the other fuels, methanol presents several advantages for hydrogen production. The

* **Corresponding author:** *email: alieliassi@yahoo.com, Tel. & Fax: #982156276637*

absence of a strong C–C bond facilitates the reforming of methanol at low temperatures (200–300 °C). This range of temperature is very low when compared to the other common fuels such as methane, which is reformed above 500 °C [2] and ethanol, with a reforming temperature around 400 °C [3]. Although methanol is highly toxic and miscible in water, it has the advantage of being biodegradable, liquid at atmospheric conditions and has high hydrogen to carbon ratio [4]. In addition to the overall methanol steam reforming (MSR) reaction, Eq. (1), two side reactions are commonly considered: methanol decomposition, Eq. (2), and water–gas shift (WGSR), Eq. (3):

$$CH_3OH + H_2O \leftrightarrow 3H_2 + CO_2 \quad \Delta H^{\circ}_{298} = +49.4\ kJ/mol \qquad (1)$$

$$CH_3OH \leftrightarrow CO + 2H_2 \quad \Delta H^{\circ}_{298} = +92\ kJ/mol \qquad (2)$$

$$CO + H_2O \leftrightarrow CO_2 + H_2 \quad \Delta H^{\circ}_{298} = -41.1\ kJ/mol \qquad (3)$$

Even though the purpose of the methanol steam reforming reaction is the production of hydrogen, there are other products formed that must be considered. Besides the non-reacted water and methanol, the reaction mixture is composed by hydrogen, carbon dioxide and small amounts of carbon monoxide. For PEM fuel cell applications, the formation of carbon monoxide must be minimized [5]. More specifically, its higher limit must be lower than 10 ppm, otherwise it poisons the anodic catalyst of the low temperature fuel cells such as PEMFC. This highlights the importance of the catalyst performance in the reaction. Ideally, the catalyst should be highly active in order to achieve large amounts of hydrogen, highly selective so that the carbon monoxide produced is negligible and finally it should present long term stability. Copper-based catalysts are the most commonly used for the MSR reaction due to their high activity and selectivity [6, 7, 8].

Recently, perovskite and spinel type oxides have been identified as quite effective catalysis materials. Cu-based catalysts prepared by reduction treatment of spinel oxides such as Cu/MnO system have been showed high activity in water-gas shift reaction [9, 10]. The catalytic performance of spinel copper-oxide composites was superior to those of conventional copper catalysts [11].

On the other hand, it seems that micro-reaction technology is an appropriate technique for using in some of portable devices, since it can reduce the volume of the chemical equipment. Recently, micro-reactors have been extensively used for several catalytic and non-catalytic reactions to hydrogen production for mobile and small portable fuel-cell systems [12, 13]. In this regard, the method of catalyst coating on micro-channel reactor is very important. There are different methods for catalyst coating on surfaces such as: suspension, sol-gel deposition, hybrid method between suspension and sol-gel deposition, electrochemical deposition, electroplating, chemical vapor deposition (CVD), physical vapor deposition (PVD) and etc. [14].

The main objectives of the present work were to prepare the Cu-Zn-Ce-Al spinel catalysts, design and fabrication of a micro-channel reactor and experimental and computational fluid dynamics (CFD) studies of methanol steam reforming in the coated micro-channel reactor by the prepared catalyst for hydrogen production.

Cu-based spinel compounds were synthesized by homogeneous precipitation and sol-gel methods. Figure 1 shows a graphical abstract of the preparation methods of Cu-Zn-Al spinel catalyst with CeO_2 promoter. These compounds were characterized and discussed based on the results of X-ray diffraction (XRD), (FT-IR), (BET), scanning electron microscopy/energy dispersive X-ray spectroscopy (SEM/EDS). The catalysts were coated on micro-channels by hybrid method between suspension and sol-gel deposition and their performance were evaluated. The effects of reaction temperature, steam to carbon ratio (S/C) and weight hourly space velocity (WHSV) on methanol conversion, hydrogen and carbon monoxide production and selectivity and throughput were investigated by catalyst evaluations.

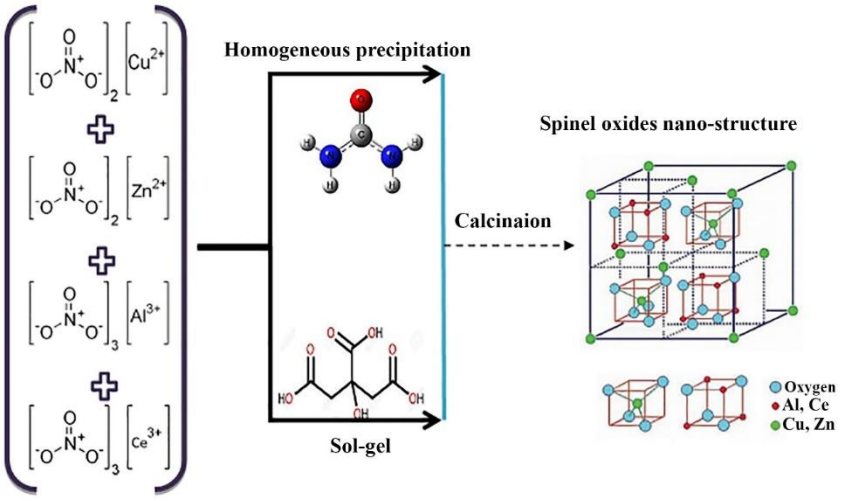

Fig. 1. Graphical abstract of preparation methods of Cu-Zn-Ce-Al spinel catalyst.

2. Experimental

2.1. Catalyst preparation

A Cu–Zn–Ce-Al spinel oxide catalyst was prepared by homogeneous precipitation (hp) of metal ions from their nitrate salt solution with an urea dilute solution by keeping temperature at 90–100 °C and constant pH=8.5-9. The obtained precipitates were aged at 60ºC for 16 h under stirring. The precipitate was centrifuged and washed with deionized water for removing the impurities. After washing, the precipitates were dried at 100°C for 16 h. Finally, the precipitates were pre-calcined at 400 °C for 1 h, and then calcined at 900 °C for 10 h in a programmable furnace with a heating rate of 5ºC/min.

Another sample of Cu-Zn-Ce-Al spinel catalyst was prepared by a sol–gel (sg) method using copper nitrate- Cu $(NO_3)_2.3H_2O$, zinc nitrate- Zn $(NO_3)_2.4H_2O$, cerium nitrate-Ce $(NO_3)_3.6H_2O$ and aluminum nitrate- Al $(NO_3)_3.9H_2O$ as precursor materials and citric acid as gelling agent. The metal precursors were mixed and dissolved in deionized water under magnetic stirring. Then another solution with molar ration 1:2 of citric acid to metal ions was added drop wise to the above solution. By adjusting the pH on 2-3 and temperature at 50 – 70 °C a dark blue wet gel was achieved. Then the wet gel was completely dried and calcined at 800 °C for 4 h.

2.2. Catalyst characterization

FT-IR spectra for the hp sample were recorded on a Philips PU 9624 (made in Germany). The spectrum is shown in the Fig. 2. This figure indicates that the selected bands in the range 400-4000 cm^{-1} are as follows: 551 (w), 695 (m), 803 (w), 1384 (s), 1635 (w), 2927 (w), 3432 (m) cm^{-1}. Based on the FT-IR result bending and stretching vibration bands of N-O and O-H bonds which appears in 1358-1537 cm^{-1} and 3300-3600 cm^{-1} wave number regions, have been removed and it indicates the lack of presence of water and nitrates in the hp catalyst.

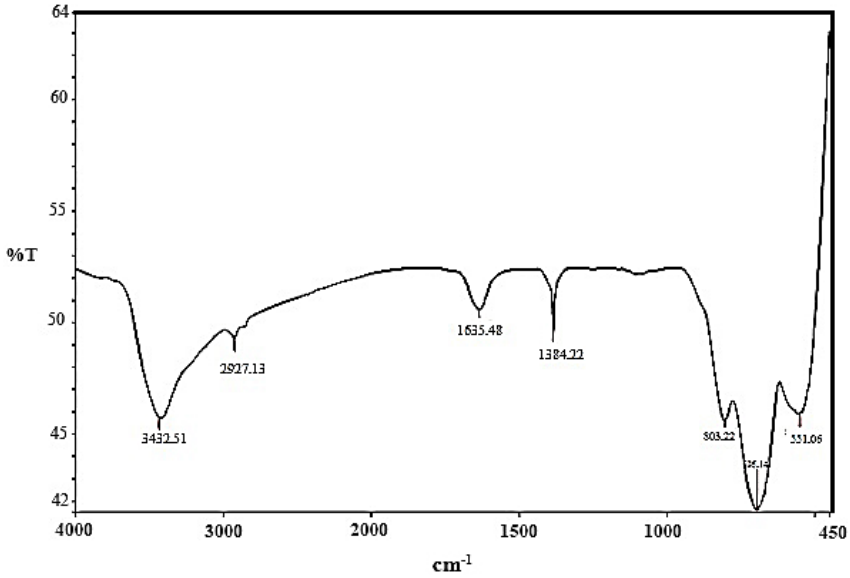

Fig 2. FT-IR Spectra for hp catalyst at 25 °C.

Thermo-gravimetric (TG) analysis was carried out by using a thermal gravimetric analysis instrument (Diamond Thermo-gravimetric, pyres) from 0-1300 ◦C. Figure 3 shows the thermal behavior of hp powder that weight loss occurs in a step at 338 ◦C such that in this temperature 35.1% of powder's weight was lost. Then with increasing the temperature to 900 ◦C, about 7% of its weight loses slowly. According to the TG results, it seems that the calcination of the powder has been occurred at 400 ◦C and then crystal structure is formed at 900 ◦C.

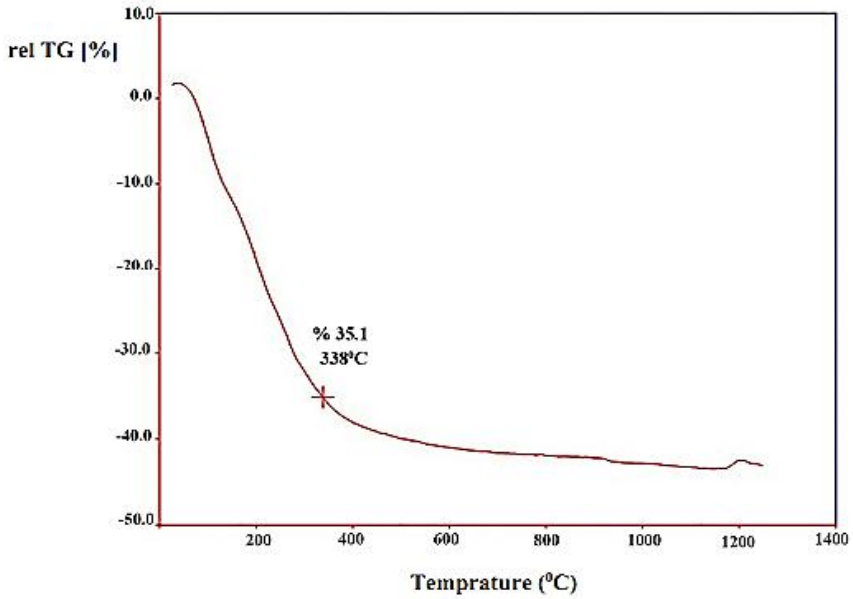

Fig 3. TG diagrams of hp catalyst before calcination.

However, if heating continue to 1200 ◦C the crystal structure may be changed. X-ray diffraction patterns were collected on a Philips X' Pert diffractometer in the -10.130-119.726 °2t range (step size = 0.032°, step time = 10 s) using the Cu Kα radiation, at a voltage of 50 kV and 40 mA of current.

Figure 4 shows XRD patterns of hp and sg catalysts. Both diffract-grams show well- defined peaks. The XRD pattern results showed the catalysts have been crystallized and they are compatible with spinel structure.

The BET analysis of the hp catalyst was obtained by N_2 adsorption–desorption data acquired at liquid N_2 temperature on a micromeritics PHS-1020(PHSCHINA).

The specific surface area and average pore diameter of the hp prepared catalyst was 39.3 m^2/g, 2.261nm, respectively. These results indicate that the hp prepared catalyst was mainly mesoporous.

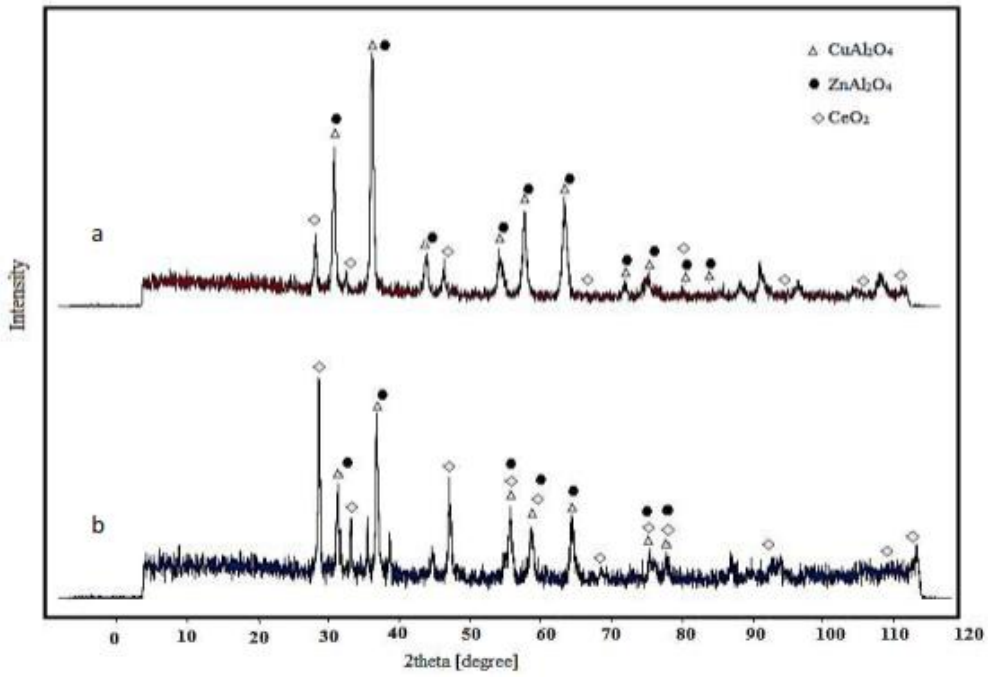

Fig 4. XRD patterns of (a) sg and (b) hp catalysts.

Also, SEM technique was used to determine the morphology and the nature of the compounds in the sg and hp catalysts. Detailed microstructure was obtained in a Philips XL30 microscope equipped with EDAX falcon energy dispersive X-ray spectrometry (EDS) unit. SEM images of the catalysts after calcination and before reduction are presented in Figure 5(a) and (b). The prepared sg catalyst revealed a granular morphology with smooth surface and the hp catalyst has spherical particles and porous structure. According to the SEM images shown in Figure 5, the average particle size of both catalysts are about 56 nm. Elemental analysis by using EDAX testified absence of impurities in the prepared catalysts.

2.3. Simulation and fabrication of micro-channel reactor

In order to evaluation of the prepared catalysts for steam reforming of methanol, a micro-channel reactor was designed and fabricated and the prepared catalysts were coated on the reactor channels by hybrid method between sol-gel and suspension methods.

It is worth noting that, flow distribution among micro-channels is an important factor affecting performance of micro-channel reactors for hydrogen production. Homogeneous flow, strongly depends on the structural design of the micro-channel reactor [15].

Mei et al. [16, 17] have proposed a flow distribution in micro-channel reactors for hydrogen production by optimization of the structural design. In their work, an innovative A-type micro-channel reactor for hydrogen production with one inlet and two outlets was developed and analyzed and effects of structural parameters on flow distribution were investigated quantitatively. Furthermore, it was found that flow distributions among the micro-channels in the A-type were much more uniform than those in the conventional Z-type micro-channel reactor with one inlet/one outlet.

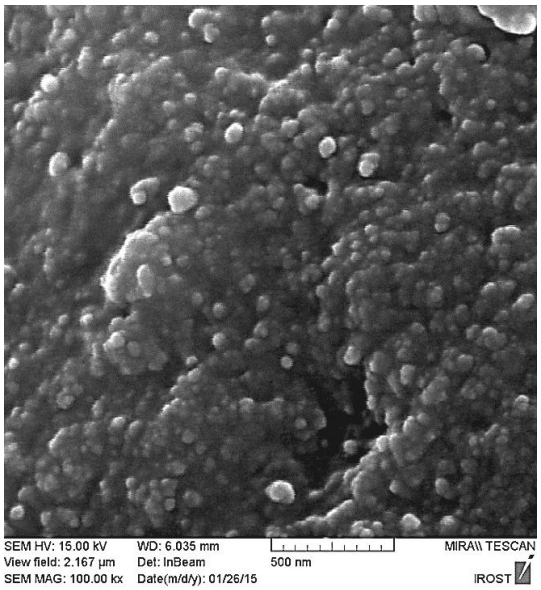

(a)

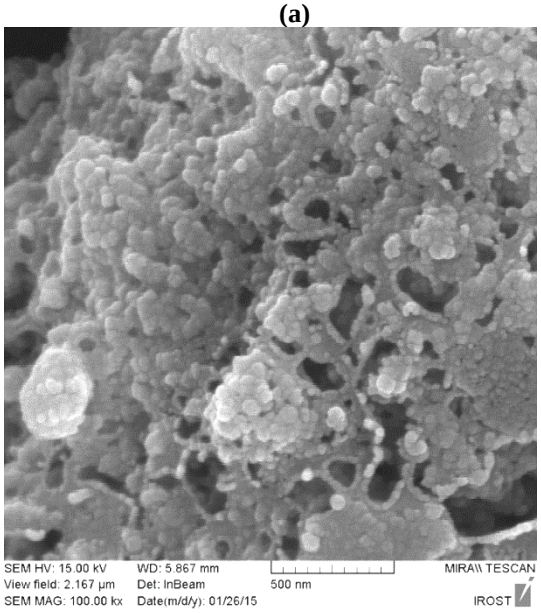

(b)

Fig 5. SEM imaging of (a) sg catalysts particles and (b) hp catalysts particles.

In the present work, two geometrical design "A" and "Z" were selected for fabrication of micro-channel reactor. Initially, by computational fluid dynamic (CFD) with Ansys CFX, the geometrical effects of micro-channels on velocity distribution for A and Z- types were considered. For both type reactors, it was assumed that the length and diameter of each cylindrical channel are 40 and 1 mm, respectively. Also, flow rate of the feed was considered 0.2684 g/s and the reactor was operated at 300ºC. For Z-type reactor, velocity distribution counter and velocity diagram for a section of the reactor in distance of 3cm of the inlet of the reactor are shown in Figure 6. According to this figure, the fluid velocity in right and left hands channels are relatively high due to the inlet and outlet effects. On the other hand, the velocity is very low in the middle channels.

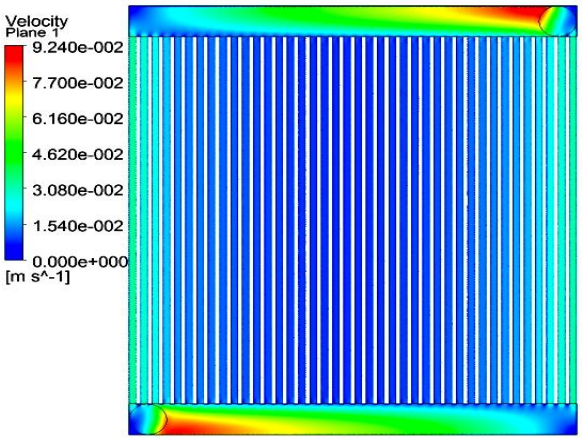

(a)

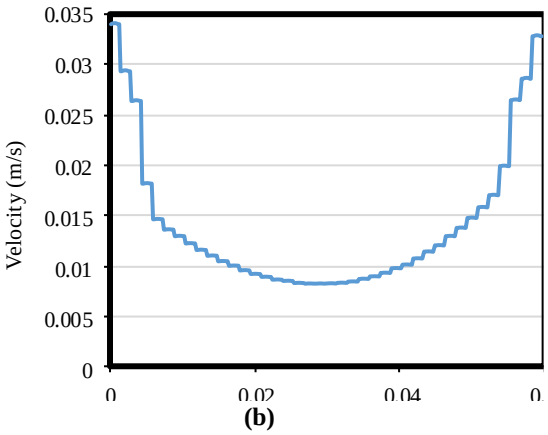

(b)

Fig 6. Velocity distribution counter (a) and velocity diagram (b) in Z- type micro-channel reactor.

The simulation results show that for this type of micro-channel, the maximum and minimum velocities were 0.034 and 0.00821 m/s, respectively. In the other word, a lot of the reactants were passed rapidly through the channels which are placed on beside of entrance and exit holes. These results are in good agreement with the experimental results those are reported by Khoshrooyan et al [18]. The same calculations were repeated for A- type micro-channel reactor. Figure 7 shows the obtained results for this reactor. It is observed that the velocity distribution for this type of micro-channels is improved in compare with Z- type and the maximum and minimum values of the velocities are reached to 0.0166 and 0.0133 m/s, respectively. In the other words, the velocity value changes in different channels are moved from 0.02579 m/s in Z- type to 0.0033 m/s in A- type reactor. Namely,

the difference between the maximum and minimum values of flow velocities is reduced to 88 percent in A-type micro-channel reactor. Therefore, it is predictable that the concentration distribution of the exit products in different channels of A- type reactor will not be wide. It should be pointed out that figure 7 shows the velocity of gases at the edges of the plate is more than the central parts. This phenomenon is due to pressure drop distribution in different channels. Actually, for special geometric shape of "A" type reactor and with notice to the inlet and outlet places of the fluid, the length of the passes fluid in beside channels are less than the central channels, therefore, the pressure drop in these channels are less than the other ones. For this reason the maximum velocity is seen at the edges.

These results are in good consistency with those were given by Mei et al [17]. So, in this work we used the A-type design for fabrication of the micro-channel reactor.

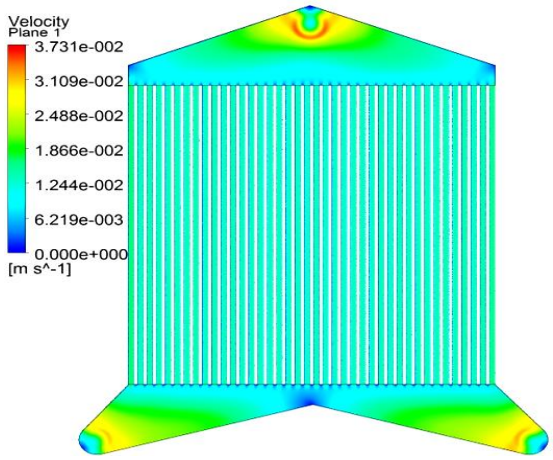

(a)

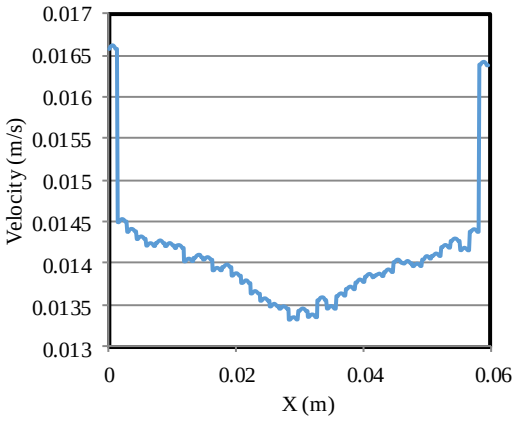

(b)

Fig 7. Velocity distribution counter (a) and velocity diagram (b) in "A" type micro-channel reactor

Our A-type micro-channel reactor was made by using titanium plate, which 40 parallel cylindrical micro-channels in this plate were made by milling and lathing process. The diameter and length of each channel were 1 mm and 40 mm, respectively. Figure 8 shows a perspective picture of the made micro-channel reactor with its jaw plates. Also, the geometrical parameters of this micro-channel reactor are reported in Table 1.

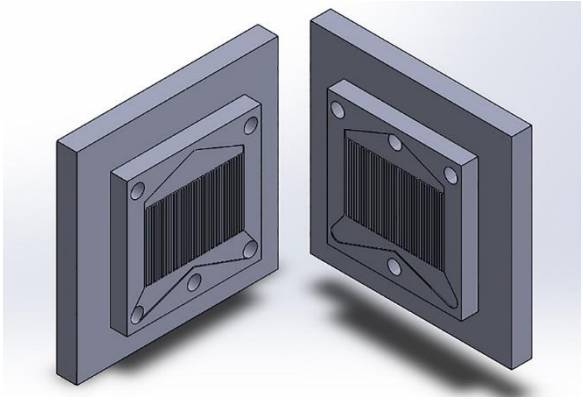

Fig 8. Perspective of the fabricated micro-channel and jaw platelets.

Table 1. Geometrical parameters of the fabricated A- type micro-channel reactor

Geometrical parameters	Value
Number of micro-channels	40
Micro-chennel lengh (mm)	40
Micro-channel diameter (mm)	1
Number of inlet holes	1
Inlet feed diameter (mm)	4
Distance from middle micro-channel to inlet (mm)	12
Number of outlet holes	2
Outlet product diameter (mm)	4
Distance from the middle channel outlets (mm)	37

2.4. Micro-channel coating

In order to coating the micro-channels, the platelets were washed with the custom methods [19]. Then, the micro-channel platelets were annealed at 300 °C for 4h at a heating rate of 10 °C/min in a furnace. This thermal treatment triggered the segregation of an alumina layer on the metallic surface. The alumina layer can help to increase the surface area and dispersion of catalytic materials.

An alumina sol was prepared by aluminum iso-propoxide, 2-propanol, ethyl cellulose and nitric acid. The sol was applied to the micro-channels of the platelets by spraying. Then the platelets were dried at 80 °C for 30 min in an

oven. The coated micro-channel platelets were calcined at 450 °C using a heating rate of 10 °C/min. The final temperature was held for 4 h.

For preparation of the catalyst slurry, the catalyst powder, ethanol, hydroxi propyl cellulose and α-therpineol were mixed and then the mixture exposed to ultrasonic waves for 20 min. In table 2 the percentage of the used chemical for preparation of the slurry is reported.

The prepared catalyst slurry was sprayed on the micro-channels with help of a spray device. Then the platelets were dried at ambient temperature in air. Subsequently, the coated micro-channel platelets were calcined at 350 °C using a heating rate of 10 °C/min. The final temperature was held for 3 h.

Table 2 - Percentage of the compounds used for the catalyst slurry preparation

Material	Percentage (%)
catalyst powder	13.7
hydroxi propyl cellulose	3.3
α-therpineol	0.137
Ethanol	82.8

Figure 9 shows the micro-channel platelets in different stages of catalyst coating. The weight of the coated catalyst was about 0.2 g and its average thickness on micro-channels was estimated about 25 µm.

The experiments for methanol steam reforming were carried out in the A-type micro-channel reactor that was coated with the prepared catalyst under atmospheric pressure. Reduction of the catalyst was carried out at 250 °C with purify H_2 (100 ml/min for 1 h). Figure 10 shows the schematic diagram of the experimental set-up.

The gas phase product was analyzed by on-line gas chromatograph (GC) (manufactured by Teyfgostar Co., Iran) using molecular sieve 5A column, thermal conductivity detector (TCD) and helium as the carrier gas. Also, methanol contents in liquid phase product were analyzed by GC using hysep Q column and flame ionization detector (FID).

Methanol conversion, H_2 and CO selectivity and throughput were defined as follows:

$$\text{Methanol conversion (\%)} = \frac{MeOH_{in} - MeOH_{out}}{MeOH_{in}} \times 100 \quad (4)$$

$$H_2 \text{ Selectivity (\%)} = \frac{F_{H_2}}{F_{CO} + F_{H_2}} \times 100 \quad (5)$$

$$CO \text{ Selectivity (\%)} = \frac{F_{CO}}{F_{CO} + F_{H_2}} \times 100 \quad (6)$$

$$\text{Throughput} = \text{Outlet gas flow rate} \times H_2 \text{ product composition} \quad (7)$$

where, F_{H_2} and F_{CO} are the effluent molar flow rates of H_2 and CO, respectively.

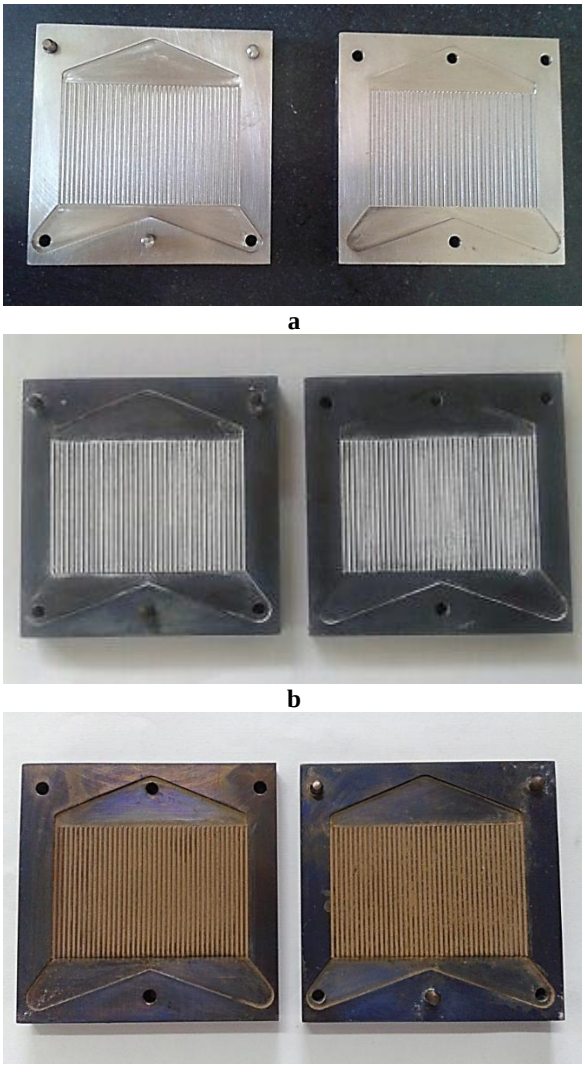

a

b

c

Fig 9. Microchannel platelets (a) after cleanup (b) after sol deposition (c) after catalyst deposition.

2.5. Catalytic activity

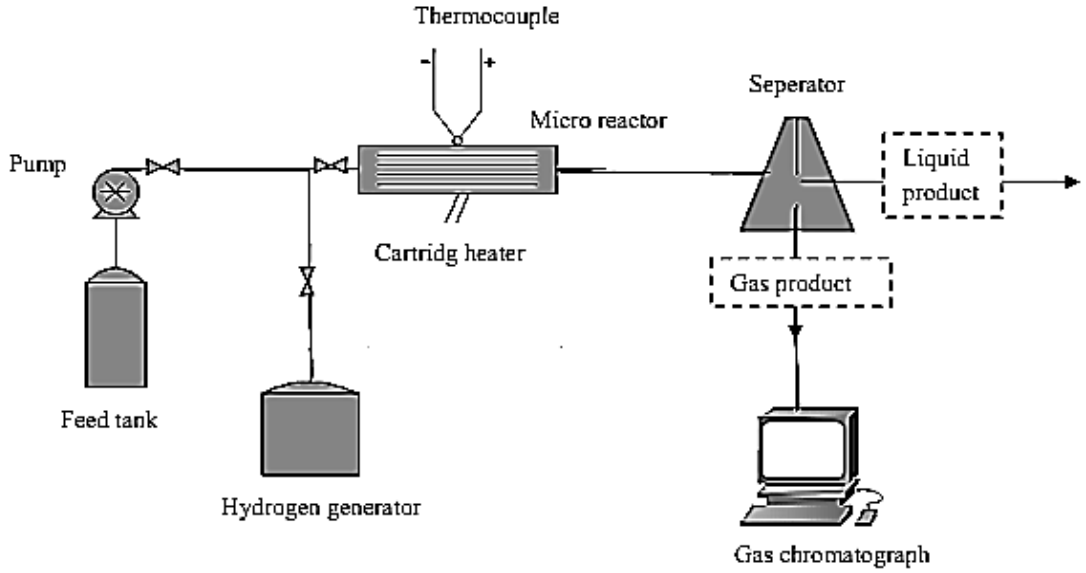

Fig 10. Schematic diagram of the experimental setup.

3. Results and discussion

For measuring the activity of two prepared catalysts (sg and hp), some experiments were carried out at different temperatures, weight hourly space velocities (WHSVs) and steam to carbon molar ratio. Figure 11 shows the reaction temperature effects on the CO and H_2 gas composition. According to the obtained results, by increasing the reaction temperature, the yield of H_2 and CO was increased for both of catalysts.

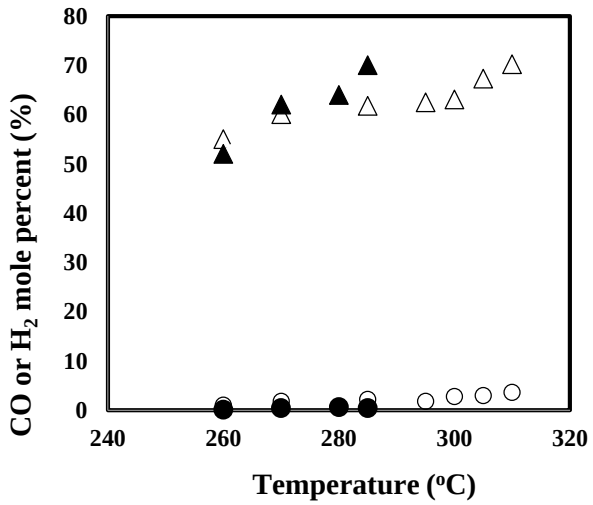

Fig 11. Effect of temperature on the performance of MSR (S/C = 2.5, WHSV=9h-1) in the A-type micro-channel reactor coated with synthesized sg and hp catalysts. CO (●) and H2 (▲) experimental mole percent for hp catalyst and CO (○) and H2(Δ) mole percent for sg catalyst.

The influence of reaction temperature on the CO and H_2 selectivity is shown in Figure 12. According to this figure, increasing the reaction temperature from 260 up to 310 °C has not any considerable effect on H_2 and CO selectivity for both of catalysts. The both prepared catalysts show high H_2 selectivity in compare with the CO selectivity.

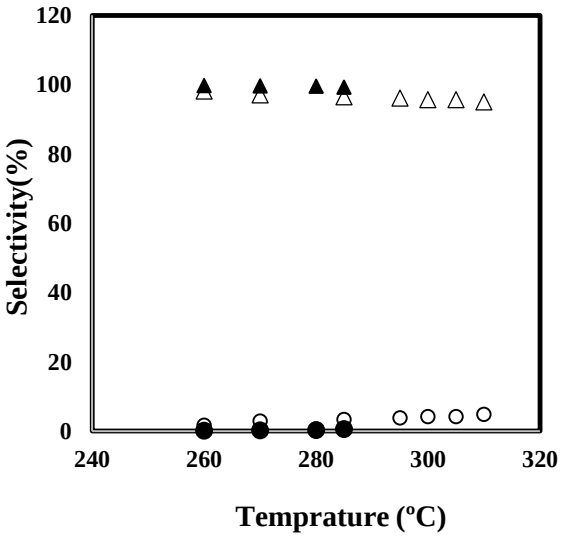

Fig 12. Effect of temperature on the H2 and CO selectivity (S/C = 2.5, WHSV=9h-1) in the A-type micro-channel reactor coated with synthesized catalysts. Solid triangles and circles are H2 and CO selectivity, respectively for sg catalyst and empty ones are for hp catalyst.

Figure 13 shows the temperature effect on methanol conversion by using two different synthesized catalysts. According to this figure methanol conversion is increased by temperature increasing. Also, methanol conversion by

using hp catalyst is more than the other catalyst at the same temperatures.

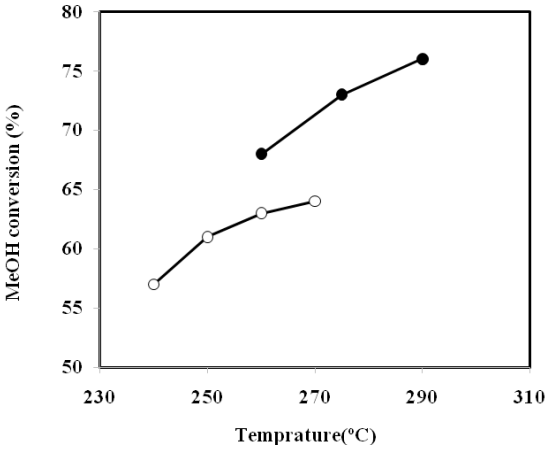

Fig 13. Effect of temperature on methanol conversion (S/C = 2.5, WHSV=9h^{-1}) in A-type micro-channel reactor coated with synthesized catalysts. Solid and empty circles are methanol conversions for hp and sg catalysts, respectively. Solid lines show the trend of changes.

Figure 14 shows the effect of temperature on throughput. It can be observed that the value of throughput for the sg catalyst is higher than the other one (hp).

In Figure 15 CO and H_2 product compositions versus WHSV at 270 °C are shown. According to this figure, the CO and H_2 concentration declined gradually with increase of WHSV, which is obvious.

It is evident from Figure 16 that the methanol conversion and throughput are increased by S/C molar ratio increasing in the A-type micro-channel reactor coated with hp synthesized catalyst. According to this figure by increasing steam to carbon molar ratio (S/C) methanol conversion and through put is increased.

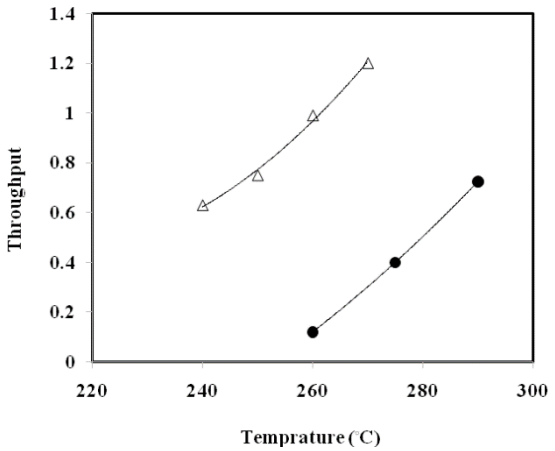

Fig 14. Effect of temperature on Throughput (lit H_2/h) of MSR in A-type micro-channel reactor coated with hp (●) and sg (○) synthesized catalysts (S/C = 2.5, WHSV= 9 h^{-1}). Solid lines indicate the trend of changes.

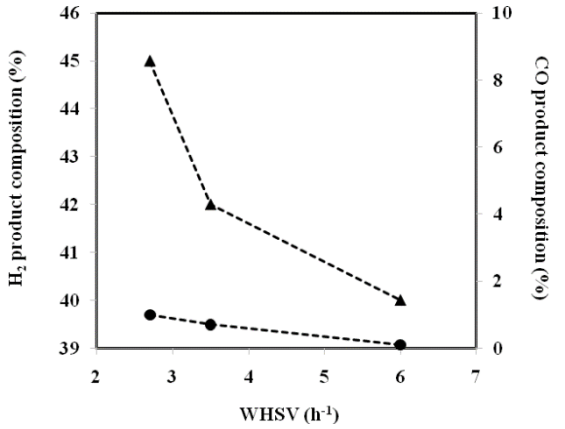

Fig 15. Effect of WHSV on the H_2 (▲) and CO (●) compositions in the A-type micro-channel reactor coated with sg synthesized catalysts (S/C = 2.5, T = 270 °C).

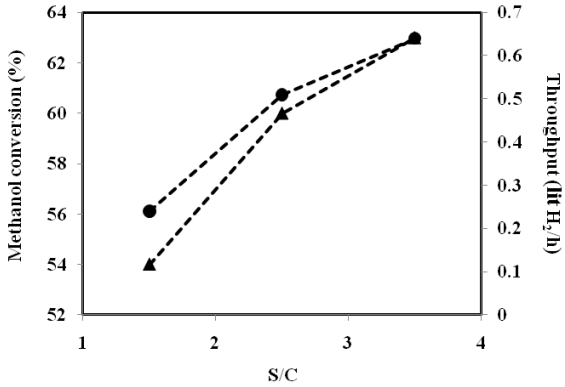

Fig 16. Effect of S/C on the methanol conversion (▲) and H_2 through put (●) of MSR in the A-type micro-channel reactor coated with hp synthesized catalyst (WHSV = 9 h^{-1}, T = 270 °C). Dashed lines show the trend of changes

Conclusion

In this work, preparation of two new Cu-Zn-Al spinel catalysts with CeO_2 as promoter by using homogeneous precipitation and sol-gel methods is reported. Both catalysts have spinel structure according to the X-ray diffraction results. Elemental analysis by using EDAX testified absence of impurities in the prepared catalysts. The scanning electron imaging (SEM) showed particles of catalysts are porous and spherical with sizes of 24-57 nm. By considering BET analysis, the surface area of the catalyst which was prepared by homogeneous precipitation method has been obtained about 39.27 m^2/g. Two geometrical shape, namely, Z and A- type for design and fabrication of a micro-channel reactor were selected. The obtained results from hydro dynamical investigations by CFD calculations for the two geometrical designs showed the A- type is preferred to Z- type because of the better fluid velocity distribution.

For evaluation of the synthesized catalyst for steam reforming of methanol it was coated on the fabricated A-type mico-channel reactor by hybrid method between sol-gel and suspension methods. The catalysts were coated on channels by spraying method and its thickness on micro-channels was about 25 microns. Different experiments were carried out by changing water to methanol molar ratio, WHSVs and temperatures for two synthesized and coated catalysts. The obtained results show that the prepared catalysts are appropriate for producing a rich H_2 gas with a low concentration of CO. Also, the catalyst which was prepared by homogeneous precipitation method (hp) exhibits the highest methanol conversion with the lowest CO concentration in the outlet gas product in compared with the other catalyst. Both catalysts give similar H_2 production yield. Also, the obtained results show that reaction temperature increasing has not any considerable effect on H_2 and CO selectivity. But it can increase the H_2 and CO production yield, methanol conversion and throughput. Finally, the experiments show that the concentration of H_2 and CO in the gas product are decreased by WHSV increasing.

Acknowledgment

The authors thank Iranian National Science Foundation (INSF) for financial support of this work. Also, authors thanks Hydrogen, Fuel Cell & Catalyst Laboratory of Chemical Technologies department of IROST.

References:

[1] S. Sá, H. Silva, L. Brandão, J.M. Sousa, A. Mendes, Appl. Catal. B: Environmental, **99** (2010) 43-57.

[2] Y. Chen, Y. Wang, H. Xu, G. Xiong, J. Membr. Sci., **322** (2008) 453-459.

[3] C. Zhang, Z. Yuan, N. Liu, S. Wang, Fuel Cells, **6** (2006) 466-471.

[4] A. Basile, A. Parmaliana, S. Tosti, A. Iulianelli, F. Gallucci, C. Espro, J. Spooren, Catal. Today, **137** (2008) 17-22.

[5] B. Lindström, L. J. Pettersson, Int. J. Hydrogen Energy, **26** (2001) 923-933.

[6] S. T. Yong, C. W. Ooi, S. P. Chai, X. S. Wu, Int. J. Hydrogen Energy, **38** (2013) 9541-9552.

[7] A. Iulianelli, P. Ribeirinha, A. Mendes, A. Basile, Renew. Sustainable Energy Rev., **29** (2014) 355-368.

[8] S. K. Talkhoncheh, M. Haghighi, M. Abdollahifar, H. Ajamein, J. Appl. Chem., **30** (2014) 89-102.

[9] J. Papavasiliou, G. Avgouropoulos, T. Ioannides, J. Catal., **251** (2007) 7-20.

[10] Y. Tanaka, T. Takeguchi, R. Kikuchi, K. Eguchi, Appl. Catal. A: General, **279** (2005) 59-66.

[11] Y.H. Huang, S.F. Wang, A.P. Tsai, S. Kameoka, Ceramics International, **40** (2014) 4541-4551.

[12] G. Kolb, Chem. Eng. Process: Process Intensification, 65 (2013) 1-44.

[13] W. Zhou, W. Deng, L. Lu, J. Zhang, L. Qin, S. Ma, Y. Tang, Int. J. Hydrogen Energy, **39** (2014) 4884-4894.

[14] V. Meille, Appl. Catal. A: General, **315** (2006) 1-17.

[15] J. M. Commenge, L. Falk, J.P. Corriou, M. Matlosz, AIChE J., **48** (2002) 345-358.

[16] D. Mei, L. Liang, M. Qian, X. Lou, Int. J. Hydrogen Energy, **38** (2013) 15488-15499.

[17] D. Mei, L. Liang, M. Qian, Y. Feng, Int. J. Hydrogen Energy, **39** (2014) 17690-17701.

[18] L. Khoshrooyan, A. Eliassi, M. Ranjbar, J. Particle Sc. Tech., **2** (2016) 41-47.

[19] J. Bravo, A. Karim, T. Conant, G.P. Lopez, A. Datye, Chem. Eng. J., **101** (2004) 113-121.